

Roll pass design for round and square sections using an informed artificial neural network

OVERHAGEN Christian^{1,a*} and MARTIN Robert^{2,b}

¹University of Duisburg-Essen, Faculty of Engineering, Institute for Technologies of Metals, Chair of Metallurgy and Metal Forming, Forsthausweg 2, 47057 Duisburg, Germany

²University of Duisburg-Essen, Faculty of Engineering, Institute for Technologies of Metals, Forsthausweg 2, 47057 Duisburg, Germany

^achristian.overhagen@uni-due.de, ^brobert.martin@uni-due.de

Keywords: Rod Rolling, Bar Rolling, Neural Networks, Roll Pass Design, Machine Learning, Custom Loss Function

Abstract. Nowadays, the roll pass design process for hot rolling mills of full sections like round and square sections is carried out by FEM simulations or analytical calculations. Both techniques require a highly iterative method with numerous iterations required to determine a satisfying pass design solution. In the present work, a neural network is trained for the process of roll pass design for round and square sections. The steps of data generation and training are combined by the formulation of a custom loss function for the underlying physical problem. In this way, the neural network is informed about the metal forming problem, enabling the generation of the necessary training data to be carried out implicitly during training. This technique increases the flexibility and extensibility of the current approach, eliminating the necessity of external training data generation. The metal forming equations for the pass design problem are presented for the pass sequences round-oval-round, as well as square-diamond-square, which are included in custom loss functions for the neural networks. The prediction results are compared to analytical iterative calculations, indicating very good agreements. Therefore, multiple iterations and computation time can be saved when the new approach of pass design is applied.

Introduction

Roll Pass Design of full sections like round and square sections is a task which is carried out to a big extent within the mill building and rolling mill industries. Therefore, we seek for methodologies which allow this process to be completed fast and accurately. Classical approaches require numerous iterations, starting from simple initial conditions for the groove design, which are refined step by step to finally yield a satisfactory solution. Balan et al. presented surrogate models for the flat rolling process based on neural networks [1] to increase the efficiency of numerical simulations. A new surrogate method for roll pass design was presented in [2], where an artificial neural network was trained with classically precalculated roll pass designs. There, the task was split into two parts, the data generation, and the training of a suitable neural network. The present approach follows a different route. Instead of utilizing a classical neural network with a default loss function provided by the machine learning framework (here: PyTorch [3]), we leverage the metal forming equations governing the pass design procedure as a custom loss function during training of the neural network. Therefore, the tedious and computationally expensive procedure of an iterative pre-calculation of the final pass design is no longer necessary. Instead, the synthetic data is generated on-the-fly during the training procedure. In the beginning, we only need to define the data range in which the neural network should be trained. Everything else will be handled by the loss function.



A roll pass design of square or round sections consists of a series of two-pass sequences, each consisting of an oval or diamond groove in the first pass (the so-called minor groove), and a round or square groove in the second pass (the so-called major groove). Usually, the sequence of major grooves in a pass design is predefined, and the task of the pass designer is to find the necessary geometries of the minor grooves. This is a highly iterative technique, requiring multiple evaluations of the same equations. In the present approach, we introduce a method to replace this procedure by direct prediction of the minor groove geometries by an artificial neural network.

The analytical formulation of the pass design problem

Since optimization techniques used for training of neural networks are generally based on gradient descent methods, the loss function of the neural network must be and differentiable. Therefore, we must find analytical expressions for the lateral spreading problem of section passes.

To calculate the groove filling by lateral spread of given groove geometries, a suitable spreading model for flat passes must be applied in conjunction with an equivalent pass method as to enable the spread calculation of section passes. For the spread calculation, we will use Roux’s spreading model as given in [5, 6]. For the transformation between the section passes and equivalent flat passes, we use an extension of the equivalent pass method by A.E. Lendl [7], which will be shown in the following.

Lendl’s method defines the mean entry and exit heights of the equivalent flat pass according to the relations

$$h_{0L} = \frac{A_{0L}}{w_i} \quad \text{and} \quad h_{1L} = \frac{A_{1L}}{w_i} . \tag{1}$$

The areas A_{0L} and A_{1L} are the parts of the entry and exit cross sections A_0 and A_1 which are subjected to the direct pressure exerted by the top and bottom roll.

A_{0L} and A_{1L} can be constructed graphically or calculated from geometrical considerations of the pass geometries. Additionally, we must define a working roll diameter, which is given by

$$d_{work} = d_{nom} - h_{1L} + s \tag{2}$$

In Eq. 2, d_{nom} is the nominal barrel diameter of the rolls and s is the roll gap of the groove.

The pass sequence round-oval-round. Fig. 1 shows the pass round-to-oval with the geometrical parameters d_0 (entry diameter), h_{ov} (height of the oval and, r_{ov} (radius of the oval).

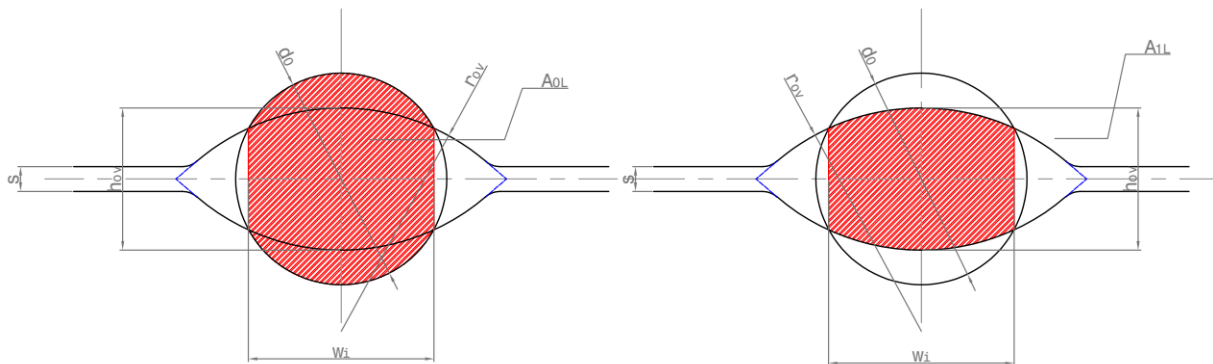


Fig. 1. The construction of the equivalence areas A_{0L} (left) and A_{1L} (right) for the pass round-to-oval.

In the present approach, we restrict our considerations to the single-radius oval, noting that the approach can be extended to multi-radius ovals as long as their geometry can be described analytically. The intersection width w_i is the distance between the intersection points of the entry section and roll contours (see Fig. 1). From geometrical considerations, it follows that

$$w_i = 2 \sqrt{r_{ov}^2 - \left(\frac{d_0^2 - 2r_{ov}^2 + h_{ov}r_{ov} - \frac{h_{ov}^2}{4}}{h - 2r_{ov}} \right)^2} \quad (3)$$

The areas A_{0L} and A_{1L} can then be calculated via

$$A_{0L} = w_i d_0 - 2w_i \frac{d_0}{2} + w_i \sqrt{\frac{d_0^2}{4} - \frac{w_i^2}{4}} + \frac{d_0^2}{2} \arcsin\left(\frac{w_i}{d_0}\right) \quad (4)$$

and

$$A_{1L} = w_i h_{ov} - 2w_i r_{ov} + w_i \sqrt{r_{ov}^2 - \frac{w_i^2}{4}} + 2r_{ov}^2 \arcsin\left(\frac{w_i}{2r_{ov}}\right) \quad (5)$$

The mean heights of the equivalent flat pass are then calculated from Eq. 1. From the spread model, the exit width of the oval section $w_1 = w_{os}$ is then calculated, from which the output oval contour is constructed.

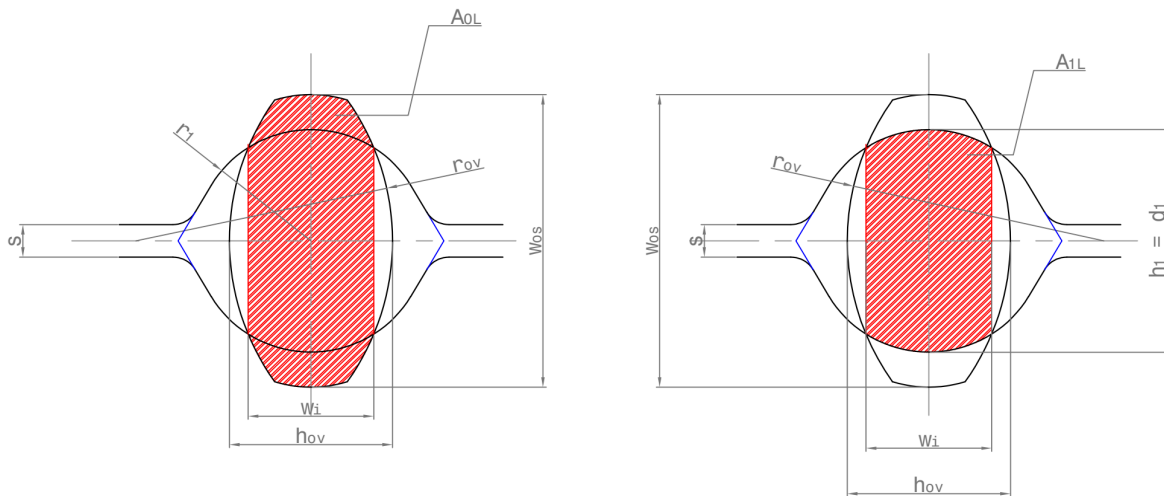


Fig. 2. Construction of the equivalence areas A_{0L} (left) and A_{1L} (right) for the pass oval-to-round.

For the second pass oval-to-round, the oval section will be rotated by 90° to an upright position and fed into a round groove. It should be noted that due to the upright rotation, the former width of the oval w_{os} now becomes the initial height, whereas the former height of the oval h_{ov} becomes the initial width. For clarity, we retain the definitions shown in Figs. 1 and 2.

In the round pass, the height of the section is reduced from w_{os} to $h_1 = d_1$ (see Fig. 2). The final radius of the round section is r_1 . We shall note that the round groove is tangentially opened to prevent rolling faults due to spreading variations. The intersection width w_i of this pass is now given as

$$w_i = \frac{h_{ov}}{2} - r_{ov} + \sqrt{r_{ov}^2 - y_i^2}, \tag{6}$$

where

$$y_i = \sqrt{r_{ov}^2 - \left(\frac{\frac{d_1^2}{4} - 2r_{ov}^2 + h_{ov}r_{ov} - \frac{h_{ov}^2}{4}}{h_{ov} - 2r_{ov}} \right)^2} \tag{7}$$

is the y-coordinate of the intersection point. Therefore, the area A_{0L} follows to (cf. Fig. 2):

$$A_{0L} = w_{os} - h_{ov} - 2w_{os}r_{ov} + w_{os}\sqrt{r_{ov}^2 - \frac{w_{os}^2}{4}} + 2r_{ov}^2 \arcsin\left(\frac{w_{os}}{2r_{ov}}\right) - \left[2y_i(h_{ov} - w_i) - 4r_{ov}y_i + 2y_i\sqrt{r_{ov}^2 - y_i^2} + 2r_{ov}^2 \arcsin\left(\frac{y_i}{r_{ov}}\right) \right] \tag{8}$$

and the area A_{1L} is:

$$A_{1L} = w_i\sqrt{\frac{d_1^2}{4} - \frac{w_i^2}{4}} + 2\left(\frac{d_1^2}{4}\right) \arcsin\left(\frac{w_i}{d_1}\right). \tag{9}$$

The equivalent heights h_{0L} and h_{1L} are again calculated by Eq. 1. Now, with the working roll diameter calculated according to Eq. 2, we can carry out the spread calculation for the second pass oval-to-round using Roux’s spreading model, yielding the final width w_2 of the round section.

As a result of the spread calculation, the final width of the round section is found. To assess the suitability of the present oval geometry, we express the filling condition of both grooves (oval and round) in terms of a filling ratio given as $f_{fill} = \text{actual width} / \text{nominal width}$. The nominal width is defined differently depending on the groove type.

For round grooves, we usually take the diameter of the intended round section as the nominal width. For minor grooves, the width on face of the minor groove is used as the nominal width. The width on face w_{of} of a single-radius oval groove is calculated according to

$$w_{of} = 2\sqrt{r_{ov}^2 - \left(r_{ov} - \frac{h_{ov} - s}{2}\right)^2}. \tag{10}$$

For non-final round sections, target filling ratios between 0.95 and 0.98 are used, while for single-radius ovals, the target filling ratios area usually in the range between 0.8 and 0.9.

The pass sequence square-diamond-square. To work out the geometrical relations leading to the definition of the equivalence areas A_{0L} and A_{1L} on the general pass diamond-to-diamond, we shall first treat the definition of the section area on a rolled diamond section, as given in Fig. 3.

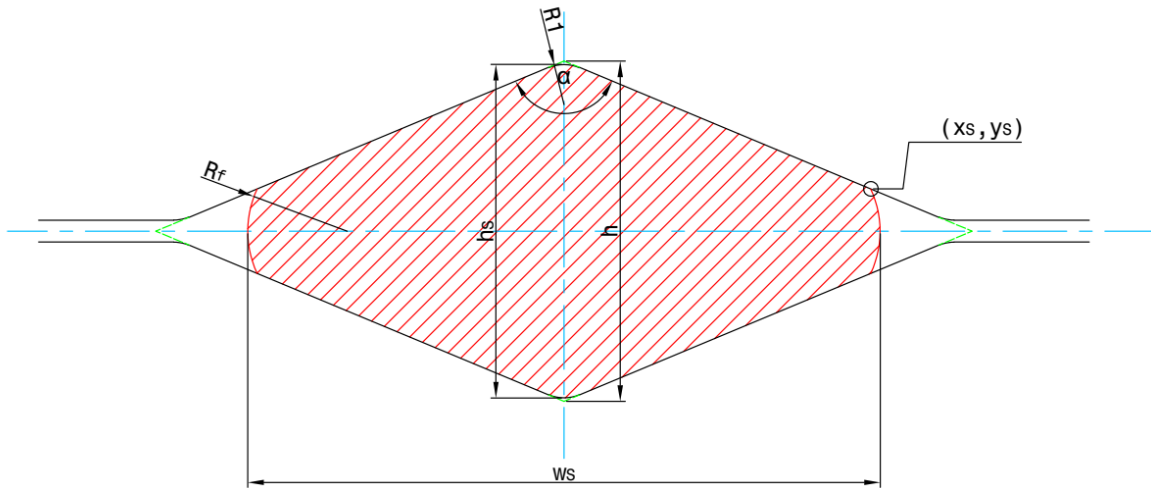


Fig. 3. Typical cross section rolled in a diamond groove.

The diamond has the theoretical height h . Practically, the groove tips are rounded with a main radius R_1 , leading to a smaller height of the exit section h_s . Under lateral spread, a final width w_s of the section is generated with the sides of the rolled section being curved at a filling radius R_f . The total area of this cross section A_S can now be calculated as follows:

$$A_S = w_s \cdot \left(h - \frac{1}{2} w_s \tan \gamma \right) - 2 \left[R_1^2 \sin^2 \gamma \tan \gamma - \frac{R_1^2}{2} (2\gamma - \sin 2\gamma) \right] - \left[(2y_s + (h - w_s \tan \gamma)) \left(\frac{w_s}{2} - x_s \right) - R_f^2 (2\phi - \sin 2\phi) \right] \quad (11)$$

Here, x_s and y_s are the coordinates of the intersection point between the arc of the filling radius and the inclined groove contour in the first quadrant (see Fig. 3). The angle ϕ corresponds to the chord of the filling radius and is given by $\tan \phi = y_s / (x_s - x_M)$, where $x_M = w_s/2 - R_f$ is the x-coordinate of the center of the radius R_f . The angle γ is always $\gamma = 90^\circ - \alpha/2$. Note that for this construction, R_f cannot be less than

$$R_{f,\min} = \frac{\frac{h}{2} - \frac{w_s}{2} \tan \gamma}{\cos \gamma - \tan \gamma (1 - \sin \gamma)} \quad (12)$$

Similarly, we can determine the equivalence areas A_{0L} and A_{1L} as shown in Fig. 4.

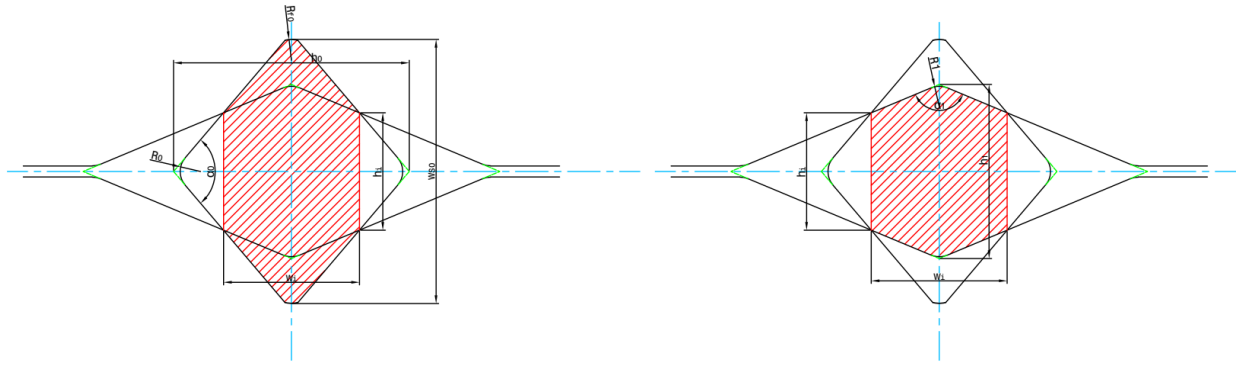


Fig. 4. The construction of the areas A_{0L} (left) and A_{1L} (right) at the generalized pass diamond-to-diamond.

In Fig. 4, the general pass diamond-to-diamond is considered, which also applies to the passes square-to-diamond and diamond-to-square as special cases. Note that the groove opening angles α_0 on the entry section, as well as α_1 of the exit section are not equal to 90° in Fig. 4 for generality of the considerations.

By comparing Fig. 4 (left) to Fig. 3 and subtracting the triangular regions left and right to the intersection distance, we can calculate the shaded area A_{0L} in Fig. 4 (left) via

$$A_{0L} = A_{0S} - \frac{h_i \cdot (h_0 - w_i)}{2} + 2R_0^2 \left[\frac{\cos^3 \frac{\alpha_0}{2}}{\sin \frac{\alpha_0}{2}} - \frac{1}{2} ((\pi - \bar{\alpha}_0) - \sin \alpha_0) \right], \quad (13)$$

where R_0 and α_0 are the original tip radius and opening angle of the entry diamond, respectively. The area A_{1L} in Fig. 4 (right) is given by

$$A_{1L} = \frac{w_i \cdot (h_1 - h_i)}{2} - 2R_1^2 \left[\frac{\cos^3 \frac{\alpha_1}{2}}{\sin \frac{\alpha_1}{2}} - \frac{1}{2} ((\pi - \bar{\alpha}_1) - \sin \alpha_1) \right] + w_i h_i. \quad (14)$$

The height and width values of the region bounded by the intersection points (see Fig. 4) are

$$w_i = \frac{h_0 \tan \frac{\alpha_0}{2} - h_1}{\tan \gamma_0 - \tan \gamma_1}, \quad (15)$$

$$h_i = h_1 - w_i \tan \gamma_1. \quad (16)$$

The passes square-to-diamond and diamond-to-square are special cases of the general case treated here, with $\alpha_0 = 90^\circ$ for square-to-diamond and $\alpha_1 = 90^\circ$ for diamond-to-square.

For the target filling criterion, we again define the width on face wof of the diamond and square grooves at the roll gap s and the groove height h by

$$wof = \tan \frac{\alpha}{2} \left(h - \frac{s}{2} \right). \quad (17)$$

In this pass sequence, we usually require a well-filled diamond groove with filling ratios of 0.95 to 0.98.

Structure of the neural network

As the roll pass design problem can be split into several units, each of which comprises a minor groove and a major groove, we design the neural network to predict the minor groove dimensions which are optimal for the transition between a given entry section (round or square) into the first pass and a given exit section out of the second pass (round or square).

We use three input features, which comprise the entry size s_0 or d_0 , the exit size s_1 or d_1 and the nominal roll diameter d_{nom} . The output features comprise the height h and width w of the minor groove to be used for the intended deformation.

It was found that a deep neural network with 3 hidden layers provided the best prediction capabilities for the current task. The first hidden layer uses 90, the second one 40 and the third hidden layer 20 neurons.

In all hidden layers, the Rectified Linear Unit (ReLU) is used as the activation function. In the output layer, we use the linear activation function as not to restrict the output data range.

Training procedure

Prior to the training, we define ranges of the input values which should be covered. Table 1 gives an overview of the training data ranges which were used for the pass design of round sections.

Table 1. Overview of the training data for the round-oval-round pass design.

	Minimum value	Maximum value	Number of values
Initial diameter d_0	15 [mm]	30 [mm]	10
Mean reduction per pass	18 [%]	25 [%]	10
Roll diameter d_{nom}	210 [mm]	500 [mm]	10

Therefore, a total of 1000 combinations of rolling parameters are considered during the training procedure. The target filling ratios are always set to 0.85 for the ovals and 0.95 for the round grooves.

The input data is normalized to a range of [0,1] for each input feature. Out of the 1000 samples, 150 are selected for the calculation of the validation loss.

A training batch size of 16 samples is used. For each batch, the neural network will propose 16 corresponding minor grooves for the intended deformation task. Based on the equations presented above, the loss function calculates the groove fillings of both passes (minor and major) and compares these values to the target filling ratios. Then, the loss function is calculated as

$$L = [w_1(h, w) - w_1^*]^2 + [w_2(h, w) - w_2^*]^2, \quad (18)$$

where w_1 and w_2 are the section widths of both passes calculated for the predicted (guessed) minor groove characterized by its height h and width w , while w_1^* and w_2^* are the target widths of the two passes.

In the beginning of the training process, the neural network will present random guesses of groove geometries to the loss function, which might lead to a non-defined loss value. Therefore, we guide the neural network towards a technically feasible range by a normalization of the output

data to a range of [0,1]. However, the outputs are not constrained to this range since we use linear activation in the output layer.

The training is carried out similarly for the square-diamond-square pass design. Table 2 provides an overview of the data ranges and the sample sizes used in the training.

Table 2. Overview of the training data for the square-diamond-square pass design.

	Minimum value	Maximum value	Number of values
Initial sidelength s_0	30 [mm]	[60] mm	10
Mean reduction per pass	20 [%]	25 [%]	10
Roll diameter d_{nom}	350 [mm]	650 [mm]	10

As a result, two trained neural networks were developed, one for the pass sequence round-oval-round and one for the pass sequence square-diamond-square. For each network training, the Adam optimization algorithm [4] is applied for 500 epochs at a learning rate of 0.0001.

Results of the neural networks and comparison to analytical calculations

The round-oval-round pass design. The neural network, trained as described above, can now be used to predict the necessary width and height values of a single-radius oval in a two-pass sequence round-oval-round.

To examine the precision of the prediction and to prove to usability of the present approach, testing data was generated using the classical iterative method on the data range given in Table 3.

Table 3. Testing data for the round-oval-round pass design neural network.

	Minimum value	Maximum value	Number of values
Initial diameter d_0	16 [mm]	29 [mm]	16
Mean reduction per pass	18 %	23 %	16
Roll diameter d_{nom}	250 [mm]	420 [mm]	16

For each of these combinations (16*16*16 = 4096 samples in total), the necessary oval groove was calculated classically using the equations (1) to (9). The calculation was repeated iteratively, until a filling error of less than 0.05 mm occurred in both passes. The neural network (trained previously using the data ranges given in Table 1) was then applied to the input data given in Table 3. The results of oval heights and widths are shown in comparison in Fig. 5.

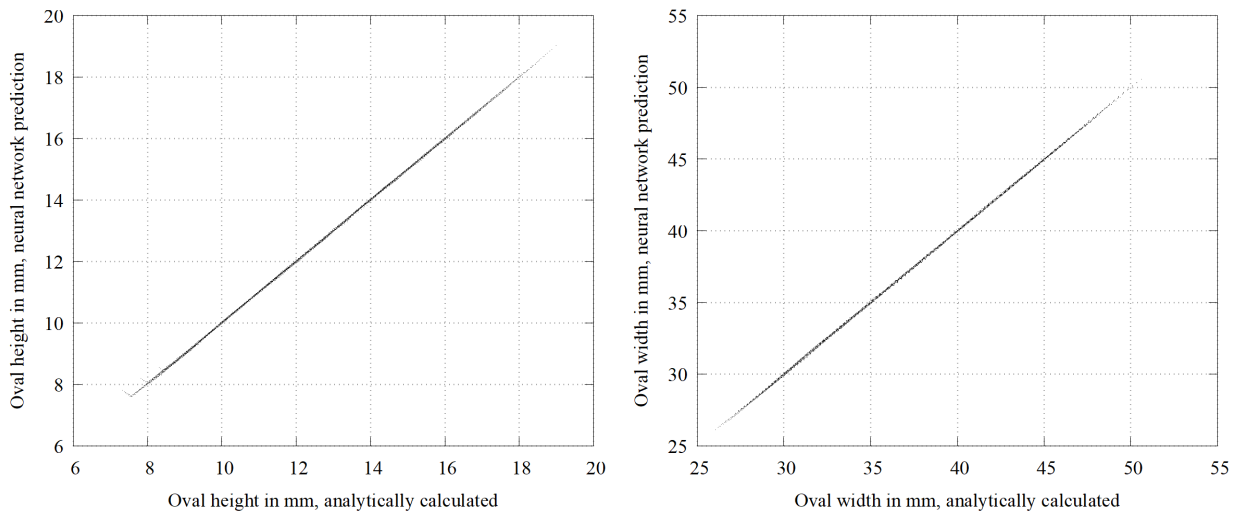


Fig. 5. Comparison of analytically calculated test data to the corresponding neural network predictions for the oval width and height.

The left-hand part of Fig. 5 shows the comparison between predicted and analytically calculated oval widths, whereas the right part of the figure shows the corresponding results for the oval heights. As can be seen, the predicted oval geometries are in very good agreement to the direct iterative calculation.

The square-diamond-square pass design. The similar procedure was carried out for the pass sequence square-diamond-square on the testing data range given in Table 5.

Table 4. Testing data for the square-diamond-square pass design neural network.

	Minimum value	Maximum value	Number of values
Initial sidelength s_0	30 [mm]	60 [mm]	16
Mean reduction per pass	20 [%]	25 [%]	16
Roll diameter d_{nom}	350 [mm]	650 [mm]	16

In Fig. 6, the prediction results of the neural network are shown in comparison to the direct analytical calculations of the pass design. Similarly as for the round-oval-round pass design, the prediction results are very close to the ones calculated analytically.

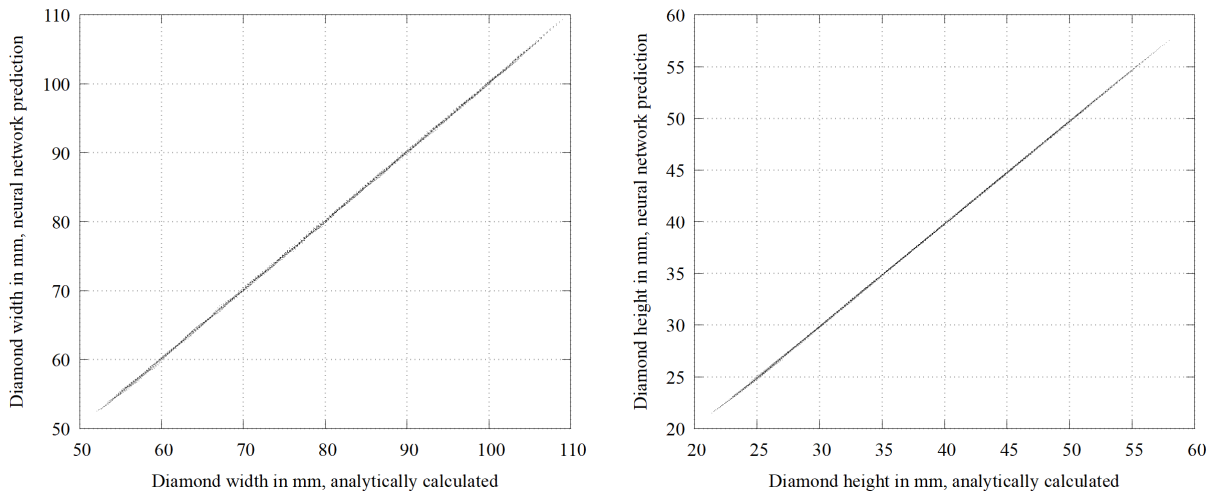


Fig. 6. Comparison of analytically calculated test data to the corresponding neural network predictions for the diamond width and height.

Checking the predictions using a numerical pass-design software. A more practical evaluation of the prediction results can be carried out when the predicted grooves are checked with a simulation and optimization software for roll pass designs. Such software solution called *MPC – Mill Process Calculations* is maintained at the Chair of Metallurgy and Metal Forming [8]. The algorithm used by the software to calculate the groove fillings is based on the same principles as the one employed as a loss function in the current approach, but not in its analytical form. Instead, a numerical treatment of the section and groove contour geometries is applied which provides a higher flexibility at the geometrical section formation.

As a study, we want to consider a pass sequence round-oval-round for an initial section with a diameter of 27 mm, to be rolled down to a final diameter of 16 mm in 4 passes at a nominal roll diameter of $d_{nom} = 300$ mm. As we see from Table 1, this data is well inside the training range of the neural network. The intermediate round diameter needed in the second pass was $d_2 = 20.66$ mm for a homogeneous deformation distribution. The two oval grooves in passes 1 and 3 were predicted by the neural network, and the groove fillings were computed using the numerical model. The cross-sectional results for the first two passes are shown in Fig. 7.

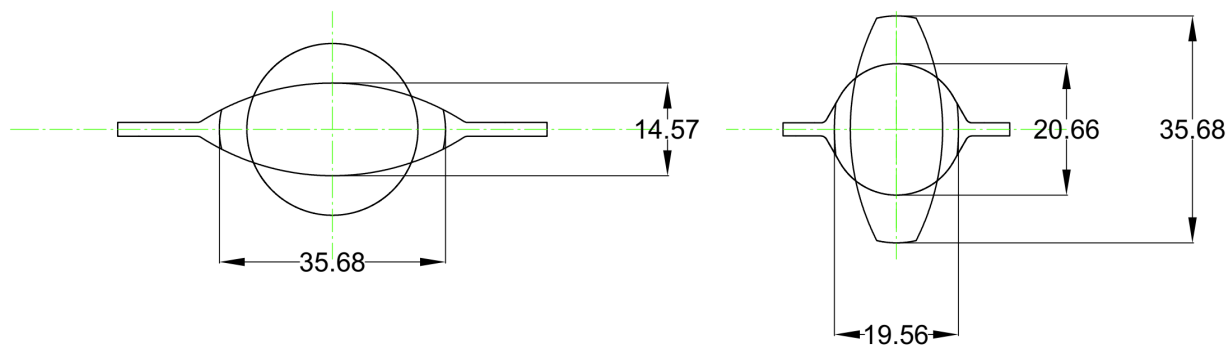


Fig. 7. Numerically calculated oval and round sections with the oval geometry proposed by the neural network for a round-oval-round sequence.

Table 5 gives an overview of the calculated results for all four passes. For the oval grooves, we define the filling ratio as the width of the section of the width on face of the groove, where the neural network was trained to design the grooves for a value of 0.85. For the round grooves, the filling ratio is defined as the section width divided by the section height. Here we trained the neural

network to reach a value of 0.95. This slight underfilling of the round grooves is intended for a good contact condition in the following oval groove within a pass sequence.

Table 5. Results of the numerical validation calculations for round-oval-round with the oval geometries proposed by the neural network.

Pass	Section shape	Height of section [mm]	Width of section [mm]	Width on face of the oval grooves [mm]	Actual filling ratio
1	Oval	14.57	35.68	41.96	0.850
2	Round	20.66	19.56		0.947
3	Oval	10.89	27.90	33.24	0.839
4	Round	16.00	15.12		0.945

Summary

In the present work, it is shown how a neural network can be informed about the metal forming equations governing the pass design process of round and square sections. The analytical model is used as a custom loss function to train a neural network for the task of roll pass design of two-pass sequences. Therefore, no pre-generated target data is used for the training, but the targets are generated by the neural network itself during the training process, based on a prescribed input data range. The data range of the network can easily be extended without the necessity of external data generation. Once trained, the neural network can predict the necessary groove geometries without the necessity of multiple iterations in close agreement to the iterative analytical calculations.

In the current usage example, we showed that the data-driven model predicts the groove geometries close to the results of analytical and numerical models. The neural network has the advantage of its easy portability compared to analytical and numerical models. Therefore, this technique is suitable to create a general method of rapid roll pass design.

Generally, artificial neural networks with custom loss functions are an interesting technique to solve systems of nonlinear equations, which can otherwise only be solved iteratively. The present roll pass design problem is only one example. However, one limitation of the approach is that the underlying physical model must be given in its analytical form, as to ensure differentiability with respect to the input parameters.

References

- [1] K. Slimani, M. Zaaf, T. Balan, Accurate surrogate models for the flat rolling process, *Int. J. Mater. Form.* 16 (2023) 23. <https://doi.org/10.1007/s12289-023-01744-5>
- [2] C. Overhagen, K. Fu, Data-Driven Roll Pass Design of Wire Rod Mills, *Key Eng. Mater.* 926 (2022) 589-601. <http://dx.doi.org/10.4028/p-dwm928>
- [3] A. Paszke, S. Gross, F. Massa, A. Lerer, J. Bradbury, G. Chanan, T. Killeen, Z. Lin, N. Gimelshein, L. Antiga, A. Desmaison, A. Köpf, E. Yang, Z. DeVito, M. Raison, A. Tejani, S. Chilamkurthy, B. Steiner, L. Fang, J. Bai, S. Chintala, PyTorch: An Imperative Style, High-Performance Deep Learning Library, arXiv: 1912.01703v1. <https://doi.org/10.48550/arXiv.1912.01703>
- [4] D.P. Kingma, J. Ba, Adam: A Method for Stochastic Optimization, arXiv: 1412.6980v9. <https://doi.org/10.48550/arXiv.1412.6980>
- [5] M.J. Roux: Etude sur le phenomene de l'elargissement dans les laminoirs, *Revue de metallurgie* 36 (1939).

- [6] P.J. Mauk, R. Kopp, Spread under Hot Rolling, *The roll pass designer* 37 (39) 3-68.
- [7] A.E. Lendl, Rolled bars – part I, *Iron and Steel* 21 (14) 397-402.
- [8] C. Overhagen, Numerical assessment of interstand tensions in continuous hot rolling processes of flat and long products, *Int. J. Adv. Manuf. Tech.* 127 (2023) 4677-4696.
<https://doi.org/10.1007/s00170-023-11584-x>